

Technical Note pubs.acs.org/synthbio

Targeted Diversification in the S. cerevisiae Genome with CRISPR-**Guided DNA Polymerase I**

Connor J. Tou, David V. Schaffer,* and John E. Dueber*



Cite This: https://dx.doi.org/10.1021/acssynbio.0c00149



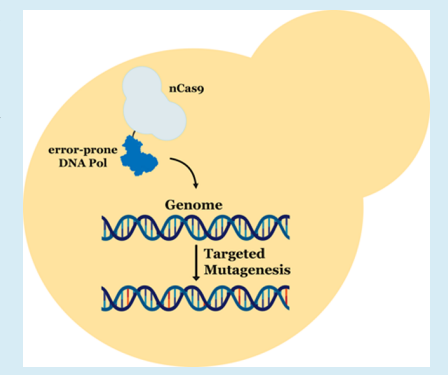
ACCESS I

Metrics & More

Article Recommendations

Supporting Information

ABSTRACT: New technologies to target nucleotide diversification *in vivo* are promising enabling strategies to perform directed evolution for engineering applications and forward genetics for addressing biological questions. Recently, we reported EvolvR—a system that employs CRISPR-guided Cas9 nickases fused to nick-translating, error-prone DNA polymerases to diversify targeted genomic loci—in E. coli. As CRISPR-Cas9 has shown activity across diverse cell types, EvolvR has the potential to be ported into other organisms, including eukaryotes, if nick-translating polymerases can be active across species. Here, we implement and characterize EvolvR's function in Saccharomyces cerevisiae, representing a key first step to enable EvolvR-mediated mutagenesis in eukaryotes. This advance will be useful for mutagenesis of user-defined loci in the yeast chromosomes for both engineering and basic research applications, and it furthermore provides a platform to develop the EvolvR technology for performance in higher eukaryotes.



KEYWORDS: CRISPR, mutagenesis, yeast, directed evolution, forward genetics, EvolvR

In vivo mutagenesis systems seek to overcome the limitations of traditional methods that rely on an unscalable and transformation-limited cycle of ex vivo diversification and in vivo selection. 1-3 The latter methods, such as traditional recombineering, are also inadequate when many adaptive mutational steps are necessary or when epistatic mutations are required for the desired phenotype. In recent work, we reported EvolvR, a system capable of diversifying all nucleotides at user-defined genomic loci in vivo.4 EvolvR works by directing error-prone, nick-translating DNA polymerases to target sequences via gRNA-directed Cas9 nickases (Figure 1a). In addition, the targeted mutagenesis rates can be tuned, and introducing fidelity-reducing point mutations into E. coli DNA polymerase I increased mutation rates up to nearly 7 orders of magnitude over that of wild type E. coli cells within a target sequence window.

EvolvR holds promise as a diversification technology that can be ported across species. For example, its translation to Saccharomyces cerevisiae would expand its capacity to facilitate forward genetics studies as well perform directed evolution of genes and regulatory elements in a native yeast context. Currently, OrthoRep, which utilizes an orthogonal error-prone DNA polymerase to replicate a cytosolically compartmentalized plasmid engineered to include a gene targeted for evolution, represents the preeminent method for continuous directed evolution of genes in yeast. However, its well-suited design to continuously diversify genes while avoiding genomic off-target effects inherently precludes the ability to diversify native chromosomal loci, which may be required for certain applications, such as forward genetics studies and strain

engineering. Additionally, it is not easily portable to other eukaryotic cell types. Yeast systems that rely on error-prone reverse transcription of a retrotransposable element⁶ are similarly not suited for applications and studies that require targeting endogenous loci. Alternatively, technologies in yeast purposed to diversify genomic segments are limited by a requirement for pre-engineered sequences to localize a mutator enzyme to the target site7 or by efficient integration of oligonucleotides libraries at replication forks, which depends on the proximity of the target site to an origin of replication as well as strain and culture conditions.8 Moreover, systems shown to function in mammalian cells are restricted to mutating only certain types of nucleotides.^{9,10} Therefore, adapting the EvolvR system to yeast (yEvolvR), to diversify all nucleotides in vivo at one or more CRISPR-targetable genomic loci, would be a biologically and biotechnologically enabling advance that would additionally establish the groundwork for EvolvR-mediated mutagenesis in higher eukaryotic cell types.

RESULTS AND DISCUSSION

yEvolvR Shows a Four Order of Magnitude Elevation in Targeted Mutation Rate. A major enabling question for

Received: March 15, 2020 Published: June 2, 2020



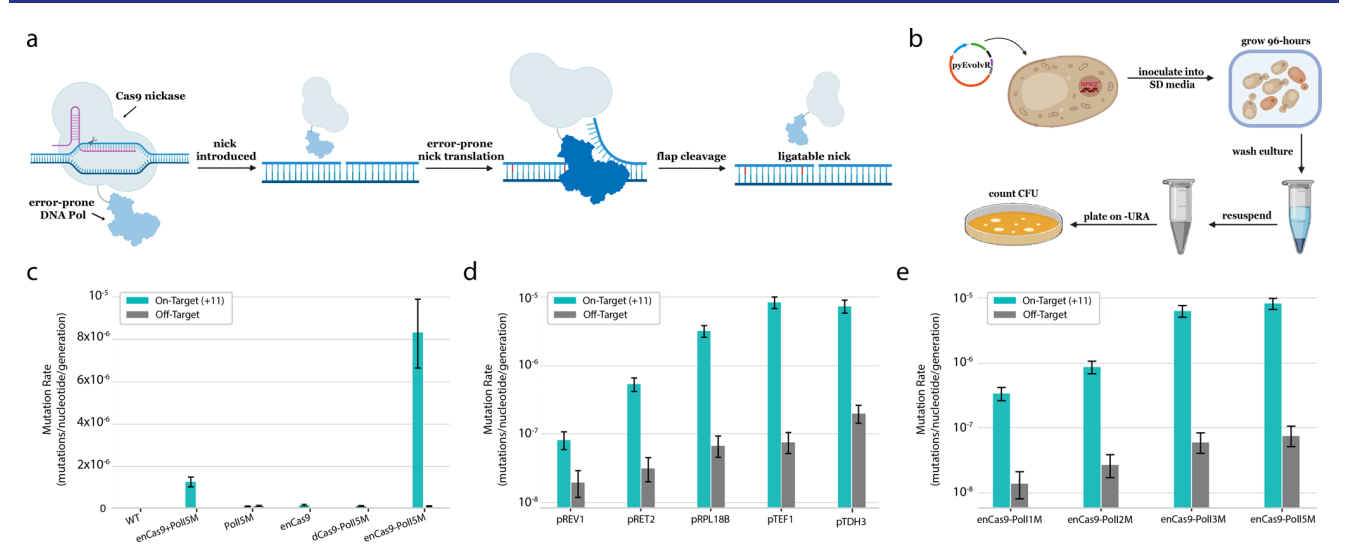


Figure 1. yEvolvR enables targeted mutagenesis at user-programmed DNA sequences. (a) yEvolvR's proposed mechanism: enCas9-mediated nicking of the target site followed by error-prone nick translation enables targeted mutagenesis at user-programmed DNA sequences. (b) Schematic of the fluctuation analysis workflow used to sensitively quantify targeted and global mutation rates. (c) The targeted and global mutation rates when expressing enCas9 and PolI5M separately, PolI5M only, enCas9 only, dCas9 fused to PolI5M, and yEvolvR (enCas9 fused to PolI5M) were determined by fluctuation analyses using an on-target guide that nicks 11 bp 5′ of a nonsense mutation in ura3* and an off-target guide targeting the HO locus. Data are the mean of eight independent biological replicates. Error bars indicate 95% confidence limits. (d) Compared to PolI5M, higher fidelity polymerases (PolI1M, PolI2M) showed lower mutation rates 11 bp from the nick. As observed in E. coli, PolI3M showed approximately the same targeted and global mutation rates at this distance. (e) With stronger promoters driving yEvolvR expression, there was an increase in targeted and global mutation rates up until pTEF1 levels. At pTDH3 levels, only global mutation rate increased.

translating EvolvR across species is whether E. coli DNA polymerase I in our original design can function in a eukaryotic cell like S. cerevisiae. To sensitively quantify the mutation rate of yEvolvR constructs while examining the function of an E. coli derived error-prone polymerase in yeast, we first adapted a fluctuation analysis assay using uracil auxotrophy (Figure 1b). A URA3 marker disabled by an ochre nonsense mutation (ura3*) was integrated into the genome of the BY4741 strain yJD053, creating the new strain yCT01. We designed a vEvolvR plasmid (pvEvolvR) to contain a guide RNA (gRNA) sequence, as described in Ryan et al. (2014), 11 and the sequence for a nicking Cas9 (D10A) variant harboring three additional mutations shown to reduce the nonspecific DNA affinity of Cas9 (enCas9)¹² fused to an *E. coli* DNA polymerase I variant harboring five fidelity-reducing mutations (PolI5M). For this assay, pyEvolvR was first transformed into yCT01. After 96 h of growth in liquid SD media selecting only for pyEvolvR, cultures were plated on SD plates lacking uracil, and mutation rates were calculated from the number of colony forming units (CFU). By fluctuation analysis, we estimated the wild type mutation rate (i.e., cells not expressing yEvolvR) at the targeted locus to be $\sim 10^{-10}$ mutations per nucleotide per generation, which agrees with previously reported values.¹³ Next, the global mutation rate (defined as the mutation rate at genomic regions not targeted by yEvolvR) was estimated from a fluctuation analysis by expressing a gRNA targeting the HO locus, which encodes an endonuclease required for the interconversion of the mating-type locus¹⁴ and has been shown to confer no growth-defect when knocked out or mutated. 15 Finally, the targeted mutation rate was determined by expressing a gRNA that enabled enCas9 nicking 11 bp 5' of the nonsense mutation in ura3*. With expression of yEvolvR (enCas9-PolI5M), the targeted mutation rate increased by 12 434-fold over wild type mutation rate, while global mutation rate increased by only 90-fold (Figure 1c). Therefore, we

concluded that PolISM was functional in the eukaryote *S. cerevisiae* and that its activity was thus not dependent on being in its native context, which will prove useful when porting EvolvR into other eukaryotic cell types. Expressing enCas9 and PolISM separately, PolISM only, enCas9 only, or dCas9 fused to PolISM showed an increase in targeted mutation rate of 1856-fold, 100-fold, 193-fold, and 133-fold, respectively, over that of wild-type, whereas the global mutation rate increased by 25-fold, 115-fold, 16-fold, and 38-fold, respectively. Thus, both the nick and PolISM are essential for yEvolvR activity. Further, localizing PolISM to the nick site *via* fusion to enCas9 increased the targeted mutation rate 7-fold over what was observed for expressing enCas9 and PolISM separately.

We sought to find the optimal yEvolvR expression level that would maximize targeted mutation rate while minimizing global mutation rate and to characterize the effect of exchanging PolI5M for other fidelity variants of E. coli DNA polymerase I on mutation rate. First, we employed a suite of promoters to drive yEvolvR transcription—pREV1, pRET2, pRPL18B, pTEF1, and pTDH3-which have been characterized to confer a 2-fold, 12-fold, 31-fold, 117-fold, and 418fold increase, respectively, in relative fluorescence units (RFU) over background when driving the expression of the fluorescent protein Venus. 16,17 We hypothesized that both targeted and global mutation rates would increase with increasing promoter strength. This was, indeed, the case up until pTEF1 levels (Figure 1d); however, increasing expression from pTEF1 to pTDH3 levels did not result in an increase in the targeted mutation rate, though the global mutation rate continued to increase. Thus, further elevation in mutation rate was not achievable through additional increases in yEvolvR expression level. Instead, further engineering of EvolvR's modular components will be required. This plateau may be due to Cas9's long residency time when bound to its target

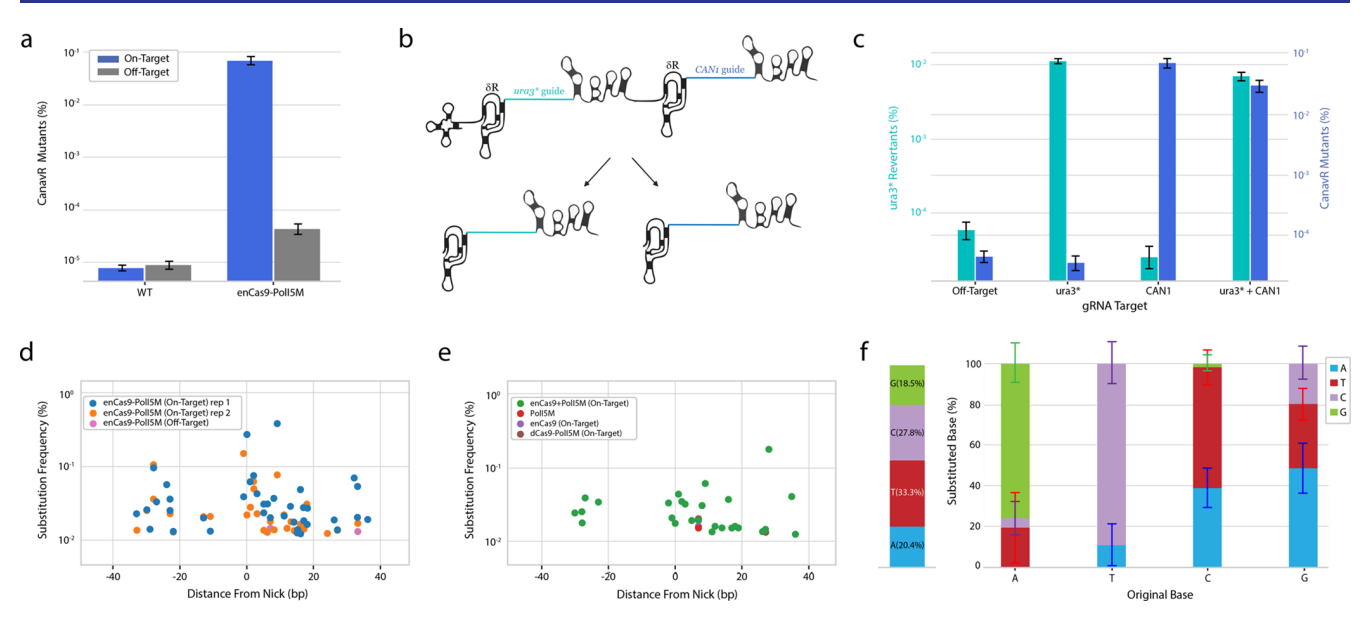


Figure 2. yEvolvR is multiplexable and generated 11 of the 12 possible substitutions within a target sequence window. (a) Targeting the endogenous *CAN1* locus and selecting for knockout mutants showed a 9019-fold increase in percent CanavR CFUs over that of wild type cells. (b) Schematic of the RNA architecture used to create two gRNAs from a single RNA transcript. One gRNA targeted *ura3** and the other targeted *CAN1*. (c) A guide targeting either *ura3**, *CAN1*, or both were expressed. Cultures were plated on both SD plates lacking uracil and SD plates lacking arginine and supplemented with 1-canavanine. Only in targeting both *ura3** and *CAN1* was a marked increase in percent *ura3** revertants and percent CanavR mutants observed. Data are the mean of eight independent biological replicates. Error bars indicate one standard deviation above and below the mean. (d) High-throughput sequencing shows that yEvolvR with an on-target guide resulted in substitutions within a 40 bp window at the targeted region. An elevation ~20 bp upstream from the nick was also observed. Expressing an off-target guide resulted in only two observed substitutions. (e) High-throughput sequencing of the condition expressing enCas9 and PolI5M separately also showed substitutions at the targeted locus. Expressing PolI5M alone, enCas9 alone, or dCas9 fused to PolI5M resulted in only one or two observed substitutions. (f) The distribution of nucleotides that were mutated by yEvolvR is displayed (left); For each of the four mutated bases, the distribution of the substituted nucleotide is shown (right). All substitutions use the target strand as reference and are derived from three independent biological replicates.

sequence. 18-20 Notably, the human Bloom syndrome helicase, BLM, as well as RNA polymerase II, have been shown to displace DNA-bound Cas9 *in vitro*, ^{21,22} and additional host factors are likely involved in dislodging Cas9 in vivo. At higher expression levels, an EvolvR molecule's initiation efficiency may become limited by how quickly a bound molecule dissociates or is displaced instead of EvolvR concentration near the target site. Our design utilizing a pTEF1 promoter thus offered an optimal balance between targeted and global mutation rates, and we continued to use pTEF1-driven yEvolvR expression for the remainder of this study. Next, we exchanged PolI5M for other fidelity variants of E. coli DNA polymerase I. As anticipated, higher fidelity polymerases with a single (PolI1M) or double (PolI2M) mutation showed lower targeted mutation rates than that of a triple mutant (PolI3M). As observed in E. coli, PolI3M showed approximately the same targeted mutation rate as PolI5M 11 bp from the nick (Figure 1e). Thus, E. coli DNA polymerase I behaved similarly as a diversifying agent in S. cerevisiae as in its native host.

yEvolvR Diversifies Endogenous Genomic Loci. As a CRISPR-guided system, yEvolvR serves as an effective method to diversify genes in their native context. We decided to target the *CAN1* locus, which encodes an arginine permease whose inactivation ablates the ability of cells to uptake arginine and its analogues. Only cells with *CAN1* disabled survive when grown on media where arginine is replaced by a toxic arginine analogue, canavanine, due to an inability to uptake canavanine.²³ Thus, *CAN1* knockout serves as a negative selection to measure yEvolvR mutagenesis at this locus. Utilizing a gRNA targeting *CAN1*, liquid cultures were plated

on SD plates lacking arginine and supplemented with L-canavanine after 96 h of growth. Canavanine resistant (CanavR) CFUs were quantified, and the percentage of CanavR mutants per viable CFU was calculated. *CAN1* targeting showed a 9019-fold increase in the percentage of CanavR mutants over that of wild type cells, while the off-target condition showed only a 5-fold increase (Figure 2a). Next, we challenged yEvolvR to diversify two genomic loci simultaneously. We expressed a single RNA transcript that self-cleaved *via* an internal HDV-ribozyme, creating two gRNA units described in Ryan *et al.* (2014)¹¹ (Figure 2b). One gRNA targeted the *ura3** locus and the other targeted the *CAN1* locus. Only in the dual gRNA condition was yEvolvR able to both revert the nonsense mutation in *ura3** and inactivate *CAN1* (Figure 2c).

Next, the targeted *CAN1* region was analyzed *via* high-throughput amplicon sequencing. As anticipated, we observed an elevation in mutagenesis within a 40 bp window in the direction of yEvolvR activity (Figure 2d). We also observed an unanticipated elevation at approximately the same frequencies within a 10–15 bp window ~20 bp from the nick site in the opposite direction of expected yEvolvR activity, which was consistent across three biological replicates. No such elevation was observed in conditions expressing only enCas9 or dCas9-PolISM, thus eliminating possibilities that this elevation in mutagenesis was solely nick-induced or that subsequent errorprone re-extension by PolISM was initiated off a pre-existing upstream nick. While further studies will seek to elucidate this mechanism, this result presents an advantage of an expanded mutagenesis window when using EvolvR in *S. cerevisiae*. Within

this window, we observed that all four nucleotides were mutated and that 11 of the 12 possible substitutions (Figure 2f), as well as indels (Figure S1), were represented in this data set containing 19 485 457 mapped reads from three biological replicates. Unsurprisingly, transition mutations made up a majority (71.3%) of the total, with 15.7%, 9.3%, 29.6%, and 16.7% constituting $A \rightarrow G$, $G \rightarrow A$, $T \rightarrow C$, and $C \rightarrow T$ mutations, respectively, using the target strand as reference (Figure S2).

CONCLUSION

Building from work previously implemented in E. coli, we have shown that the EvolvR technology can be extended to eukaryotes by demonstrating targeted mutagenesis in native chromosomal loci of S. cerevisiae. We characterized the tunability of yEvolvR by both varying expression levels and exchanging the polymerase module of EvolvR's architecture. Further efforts to engineer low fidelity polymerases with higher processivities will continue to add to an expanding EvolvR toolbox. Notably, we also uncovered a phenomenon in S. cerevisiae whereby an elevation in mutagenesis occurred both with and opposite to yEvolvR's expected directionality. This presents a useful characteristic of yEvolvR by creating an extended mutagenesis window length and represents an area for further study to better understand EvolvR's mechanism in eukaryotic cells, particularly regarding the effects of eukaryotic repair machinery. Yeast provides an excellent eukaryotic model system for investigating EvolvR function, as it offers the advantages of a short generation time, growth to large cell densities, and an abundance of genetic and synthetic biology tools. Additionally, yEvolvR should prove to be a valuable tool for facilitating the study of the genetic mechanisms underlying eukaryotic biology through forward genetics. Its ability to target multiple genomic loci simultaneously is advantageous, particularly when multiplexed diversification is essential to uncover epistatic relationships. Finally, yEvolvR establishes the feasibility of EvolvR-mediated mutagenesis in eukaryotes, thereby offering a segue to mammalian and other higher eukaryotic cells.

METHODS

Plasmid and Strain Construction. All plasmids were constructed via Golden Gate assembly. pyEvolvR consisted of yEvolvR and gRNA expression cassettes, a CEN/ARS origin of replication, and a LEU auxotrophic marker. The strain yCT01 was made by integrating a sequence containing a URA3 marker harboring an ochre nonsense mutation (S131*), a HIS auxotrophic marker, and sequences homologous to regions flanking the HIS locus into yJD053, which has genotype: his3 $\partial 1$; leu2 $\partial 0$; met15 $\partial 0$; ura3 $\partial 0$; gal2 Δ . The full plasmid sequences are listed in Table S1.

Fluctuation Analysis Assay. The strain yCT01 was transformed with 500 ng of pyEvolvR via LiOAc transformation and resuspended in 100 μ L of sterile water. 12 μ L of this suspension was inoculated into 2 mL of SD liquid medium lacking histidine and leucine. After shaking for 96 h at 30 °C, cultures were washed with sterile water and plated on SD plates lacking uracil at appropriate dilutions to allow countable CFUs. For viable CFUs, a 1:1 000 000 dilution was plated on nonselective SD plates. After 72 h of incubation at 30 °C, $ura3^*$ revertant CFUs and viable CFUs were counted. All experiments were done with eight replicates.

CAN1 Negative Selection Assay. Identical to the setup of a fluctuation analysis assay, the strain yCT01 was transformed with 500 ng of pyEvolvR. 12 μL of the cell suspension was inoculated into 2 mL of SD liquid medium lacking histidine and leucine, and cultures were allowed to shake for 96 h at 30 $^{\circ}$ C. Cultures were washed with sterile water and plated on SD plates lacking arginine and containing 60 ug/mL L-canavanine. After 72 h of incubation at 30 $^{\circ}$ C, canavanine resistant CFUs and viable CFUs were counted. All experiments were done with eight replicates.

Calculation of Mutation Rate. The R package rSalvador²⁴ was utilized to calculate mutation rates. Using data from eight independent biological replicates, the mean number of expected mutations, m, was calculated via the function newton.LD(), which computes the maximum likelihood estimate of m under the Luria-Delbruck model. Phenotypic mutation rates were calculated according to the equation $\mu = m/N_t$, where N_t is the mean number of viable cells per culture. In order to calculate per base mutation rates, the phenotypic rate was divided by the number of ways ura3* (S131*) can revert into URA3. Since all SNPs that create a missense mutation at this site are predicted to be permissive (Table S4), there are 2.33 ways this can occur from an ochre stop codon. To calculate 95% confidence limits, the function confint.LD() was utilized with alpha = 0.05, and mutation rates were calculated from these bounds.

High-Throughput Sequencing Sample Preparation. The strain yCT01 was transformed with pyEvolvR, which contained a guide targeting the CAN1 locus, and resuspended in 100 μ L of sterile water. 12 μ L of this suspension was inoculated into 2 mL of SD liquid medium lacking histidine and leucine. The cultures were grown for 96 h at 30 °C in a shaker set to 200 rpm. A YeaStar Genomic DNA kit (Zymo Research) was used to isolate genomic DNA. The oligonucleotides CAN1.NGS F and CAN1.NGS R (Table S3) were used to amplify the target region in a 15-cycle PCR reaction using 200 ng of isolated genomic DNA as template. A second, 15-cycle PCR reaction was used to add Illumina sequencing adapters and indices. The samples were then quantified by a NanoDrop 2000 spectrophotometer and submitted to the University of California, Berkeley Vincent J. Coates Genomics Sequencing Laboratory for quality control and sequencing. Quality control included fragment analysis via an Agilent 2100 Bioanalyzer, Pippin Prep, and concentration measurements by quantitative PCR. Samples were mixed in an equimolar pool and run on an Illumina NovaSeq S4 with 150 bp paired-end reads.

High Throughput Sequencing Data Analysis. Using NGMerge, ²⁵ perfectly complementary paired-end reads were merged with parameters: mismatches = 0, FASTQ quality offset score = 33, maximum input quality score = 41. Next, bowtie2 was used to align merged reads to the wild-type *CAN1* reference sequence. Samtools was utilized to generate mpileup files using parameters: minimum mapping quality score = 0, minimum base quality score = 30, maximum depth = 10 000 000. SiNPLe²⁶ was used for variant calling using parameter: theta = 0.99 (defined as the prior probability of a real variant). Variants in the resulting txt files were filtered to display only those with less than 0.01% probability of having resulted from base-calling errors.

ASSOCIATED CONTENT

5 Supporting Information

The Supporting Information is available free of charge at https://pubs.acs.org/doi/10.1021/acssynbio.0c00149.

Plasmid sequences used in this study; Promoter sequences used in this study; gRNA protospacer and oligonucleotide sequences used in this study; Amino acid sequences used in this study; Permissibility of all nonterminating mutations to the ochre nonsense mutation in *ura3**; Indel frequencies per position and indel length distribution; Distribution of the 12 possible substitutions from high throughput amplicon sequencing (PDF)

Python code used to analyze NGS data (ZIP)

AUTHOR INFORMATION

Corresponding Authors

John E. Dueber — Department of Bioengineering, University of California, Berkeley, California 94720, United States; Biological Systems & Engineering Division, Lawrence Berkeley National Laboratory, Berkeley, California 94720, United States; Innovative Genomics Institute, University of California Berkeley and San Francisco, Berkeley, California 94720, United States; Email: jdueber@berkeley.edu

David V. Schaffer — Department of Bioengineering, Department of Molecular and Cell Biology, and Helen Wills Neuroscience Institute, University of California, Berkeley, California 94720, United States; Department of Chemical and Biomolecular Engineering, University of California Berkeley, Berkeley, California 94720, United States; Innovative Genomics Institute, University of California Berkeley and San Francisco, Berkeley, California 94720, United States; Email: schaffer@berkeley.edu

Author

Connor J. Tou — Department of Bioengineering, University of California, Berkeley, California 94720, United States; Innovative Genomics Institute, University of California Berkeley and San Francisco, Berkeley, California 94720, United States; orcid.org/0000-0003-2444-4215

Complete contact information is available at: https://pubs.acs.org/10.1021/acssynbio.0c00149

Author Contributions

C.J.T. designed and performed all experiments, constructed all plasmids and strains, carried out all data analysis, and wrote the manuscript. D.V.S. and J.E.D. supervised the study and contributed to editing the manuscript.

Notes

The authors declare no competing financial interest. The plasmid encoding enCas9-PolISM (pyEvolvR) will be available from Addgene.

ACKNOWLEDGMENTS

We thank Shakked Halperin and Melanie Abrams for experimental input, Juan Hurtado for assistance in NGS data analysis, and Shana McDevitt at the University of California, Berkeley, Vincent J. Coates Genomics Sequencing Laboratory for assistance with high-throughput sequencing. C.J.T., D.V.S., and J.E.D. were supported by the Innovative Genomics Institute. C.J.T. and J.E.D. were supported by NSF grant MCB1818307.

ABBREVIATIONS

PolIxM, E. coli DNA polymerase I with x-number of stacked, fidelity-reducing mutations; enCas9, enhanced nicking Cas9 (nCas9 D10A harboring K848A, K1003A, R1060A).

REFERENCES

- (1) Esvelt, K. M., Carlson, J. C., and Liu, D. R. (2011) A system for the continuous directed evolution of biomolecules. *Nature* 472, 499–503.
- (2) Wang, H. H., Isaacs, F. J., Carr, P. A., Sun, Z. Z., Xu, G., Forest, C. R., and Church, G. M. (2009) Programming cells by multiplex genome engineering and accelerated evolution. *Nature* 460, 894–898.
- (3) Chen, H., Liu, S., Padula, S., Lesman, D., Griswold, K., Lin, A., Zhao, T., Marshall, J., and Chen, F. (2020) Efficient, continuous mutagenesis in human cells using a pseudo-random DNA editor. *Nat. Biotechnol.* 38 (2), 165–168.
- (4) Halperin, S. O., Tou, C. J., Wong, E. B., Modavi, C., Schaffer, D. V., and Dueber, J. E. (2018) CRISPR-guided DNA polymerases enable diversification of all nucleotides in a tunable window. *Nature* 560 (7717), 248–252.
- (5) Ravikumar, A., Arzumanyan, G. A., Obadi, M. K.A., Javanpour, A. A., and Liu, C. C. (2018) Scalable, continuous evolution of genes at mutation rates above genomic error thresholds. *Cell* 175, 1946–1957.
- (6) Crook, N., Abatemarco, J., Sun, J., Wagner, J. M., Schmitz, A., and Alper, H. S. (2016) *In vivo* continuous evolution of genes and pathways in yeast. *Nat. Commun.*, DOI: 10.1038/ncomms13051.
- (7) Finney-Manchester, S. P., and Maheshri, N. (2013) Harnessing mutagenic homologous recombination for targeted mutagenesis in vivo by TaGTEAM. Nucleic Acids Res. 41, e99.
- (8) Barbieri, E. M., Muir, P., Akhuetie-Oni, B. O., Yellman, C. M., and Isaacs, F. J. (2017) Precise editing at DNA replication forks enables multiplex genome engineering in eukaryotes. *Cell* 171 (6), 1453.
- (9) Ma, Y., Zhang, J., Yin, W., Zhang, Z., Song, Y., and Chang, X. (2016) Targeted AID-mediated mutagenesis (TAM) enables efficient genomic diversification in mammalian cells. *Nat. Methods* 13, 1029–1035
- (10) Hess, G. T., Frésard, L., Han, K., Lee, C. H., Li, A., Cimprich, K. A., Montgomery, S. B., and Bassik, M. C. (2016) Directed evolution using dCas9-targeted somatic hypermutation in mammalian cells. *Nat. Methods* 13 (12), 1036–1042.
- (11) Ryan, O. W., Skerker, J. M., Maurer, M., Tsai, J. C., Poddar, S., Lee, M. E., DeLoache, W., Dueber, J. E., Arkin, A. P., and Cate, J. H. D. (2014) Selection of chromosomal DNA libraries using a multiplex CRISPR system. *eLife* 3, No. e03703.
- (12) Slaymaker, I. M., Gao, L., Zetsche, B., Scott, D. A., Yan, W. X., and Zhang, F. (2016) Rationally engineered Cas9 nucleases with improved specificity. *Science* 351, 84–88.
- (13) Drake, J. W. (1991) A Constant Rate of spontaneous mutation in DNA-based microbes. *Proc. Natl. Acad. Sci. U. S. A.* 88, 7160–7164.
- (14) Winge, O., and Roberts, C. (1949) A gene for diploidization on yeast. Ser. Physiol. 24, 341–346.
- (15) Baganz, F., Hayes, A., Marren, D., Gardner, D. C., and Oliver, S. G. (1997) Suitability of replacement markers for functional analysis studies in Saccharomyces cerevisiae. *Yeast* 13 (16), 1563–73.
- (16) Lee, M. E., Deloache, W. C., Cervantes, B., and Dueber, J. E. (2015) A Highly Characterized Yeast Toolkit for Modular, Multipart Assembly. ACS Synth. Biol. 4 (9), 975–986.
- (17) Lee, M. E., Aswani, A., Han, A. S., Tomlin, C. J., and Dueber, J. E. (2013) Expression-level optimization of a multi-enzyme pathway in the absence of a high-throughput assay. *Nucleic Acids Res.* 41 (22), 10668–10678
- (18) Jones, D., Unoson, C., Leroy, P., Curic, V., and Elf, J. (2017) Kinetics of dCas9 Target Search in Escherichia Coli. *Biophys. J.* 112 (3), 314A.
- (19) Ma, H., Tu, L. C., Naseri, A., Huisman, M., Zhang, S., Grunwald, D., and Pederson, T. (2016) CRISPR-Cas9 nuclear

dynamics and target recognition in living cells. J. Cell Biol. 214 (5), 529-537.

- (20) Sternberg, S. H., Redding, S., Jinek, M., Greene, E. C., and Doudna, J. A. (2014) DNA interrogation by the CRISPR RNA-guided endonuclease Cas9. *Nature* 507, 62–67.
- (21) Zhang, Q., Wen, F., Zhang, S., Jin, J., Bi, L., Lu, Y., Li, M., Xi, X., Huang, X., Shen, B., and Sun, B. (2019) The post-PAM interaction of RNA-guided spCas9 with DNA dictates its target binding and dissociation. *Sci. Adv.* 5 (11), eaaw9807.
- (22) Clarke, R., Heler, R., MacDougall, M. S., Yeo, N. C., Chavez, A., Regan, M., Hanakahi, L., Church, G. M., Marraffini, L. A., and Merril, B. J. (2018) Enhanced bacterial immunity and mammalian genome editing *via* RNA polymerase-mediated dislodging of Cas9 from double strand DNA breaks. *Mol. Cell* 71 (1), 42–55.
- (23) Ekwall, K., and Ruusala, T. (1991) Budding yeast CAN1 gene as a selection marker in fission yeast. *Nucleic Acids Res.* 19 (5), 1150.
- (24) Zheng, Q. (2017) rSalvador: An R Package for the Fluctuation Experiment. G3: Genes, Genomes, Genet. 7 (12), 3849–3856.
- (25) Gaspar, J. M. (2018) NGmerge: merging paired-end reads via novel empirically-derived models of sequencing errors. BMC Bioinf. 19, 536.
- (26) Feretti, L., Tennakoon, C., Silesian, A., Freimanis, G., and Ribecca, P. (2019) SiNPle: Fast and sensitive variant calling for deep sequencing data. *Genes* 10, 561.